Biomed Microdevices (2010) 12:923–933
DOI 10.1007/s10544-010-9447-9

Integrated microfluidic biophotonic chip for laser induced fluorescence detection

Arvind Chandrasekaran · Muthukumaran Packirisamy

Published online: 19 June 2010

Abstract Integrated Lab-on-a-Chip or Micro-Total Analysis Systems offer several advantages for the detection of active chemical and biological species. In this work, an integrated microfluidic biophotonic chip is proposed for carrying out laser induced fluorescence detection. A Spectrometer-on-Chip device, specifically designed for multiple fluorescence detections at different emission wavelengths is integrated with the opto-microfluidic chip fabricated on Silicon-Polymer hybrid platform. The input fiber from the laser source, and output fiber coupled with a Spectrometer-on-Chip were integrated with the microfluidic channel so as to make a robust setup. Fluorescence detection was carried out using Alexafluor 647 tagged antibody particles. The experimental results show that the proposed biophotonic microfluidic device is highly suitable for high throughput detection of chemical and biological specimens.

Keywords Lab-on-a-Chip · Biophotonics · Microfluidics · Spectrometer-on-Chip · Laser-induced fluorescence · Alexafluor 647 · Hybrid integration

1 Introduction

Lab-on-a-Chip or Micro-Total Analysis Systems (μTAS) (Samel et al. 2007; Jakeway et al. 2000; Reyes et al. 2002; Auroux et al. 2002; Vilkner et al. 2004; Dittrich et al. 2006), as they are sometimes referred to as, offer several advantages for health monitoring, Point-of-Care Testing (POCT), rapid detection of biological and chemical species and bio-security, by virtue of miniaturization, portability, improved signal-to-noise ration and the ability to carry out *in-situ* medical detections. Integrated Lab-on-a-chip devices that rely on optical techniques for high sensitivity bio-detection are also known as biophotonic chips (Bettiol et al. 2006). Depending upon its application and functionality, several components can be integrated within a biophotonic chip. However, microfluidics is an essential unit of biodetection because it not only introduces the biological environment into the system but also enables convenient handling of smaller sample volumes, transportation of the fluids into the detection units and the ejection of wastes after analysis.

Monolithic integrated systems such as the device demonstrated by Burns et al. (Burns et al. 1998) are highly suitable for biophotonic chip applications. But the requirements of some macro-scale operating units, such as microfluidic pumps, lasers, spectrum analysers etc make it impossible to fabricate the ensembles monolithically, and therefore a hybrid integrated package is required to cluster such macroscale components with microfabricated devices (Krulevitch et al. 2002).

In the past, research has been carried out on the integration of micro-optical ensembles, (Seo and Lee 2004; Leistiko and Jensen 1998; Yegnanarayanan et al. 2007; Ruano et al. 2003; Chabinyc et al. 2001; Irawan et al. 2006; Su et al. 2008) within biophotonic Lab-on-a-Chip devices for various types of detection. Several biophotonic detection methods such as fluorescence (Webster et al. 2001), absorption (Balslev et al. 2006), refractometry (White et al. 2007), evanescent wave spectroscopy (Jiang et al. 2008), etc. have also been reported in the literature. Among the different biodetection techniques, Laser Induced

A. Chandrasekaran (✉) · M. Packirisamy
Optical Bio Microsystems Laboratory,
Department of Mechanical Engineering, Concordia University,
Montreal, QC, Canada
e-mail: achandra@alcor.concordia.ca

Fluorescence (LIF) spectroscopy is one of the most common techniques used for biosensing owing to its high sensitivity, selectivity, and the ability to carry out instantaneous detection, among others and the potential applications their potential applications in biophotonic Lab-on-a-Chip systems are numerous (Thrush et al. 2003).

In this work, an optical microfluidic platform hybrid integrated with Spectrometer-on-Chip is presented for fluorescence based biodetection. The proposed system incorporates a novel silicon-polymer microfluidic channel platform integrated with optical waveguides within the channels. Spectrometer-on-Chip designed specifically for the detection of particular wavelengths of fluorescence emissions has been integrated with the opto-microfluidic chip for biophotonic detections. In order to understand the feasibility of hybrid integration for fluorescence spectroscopy using the Spectrometer-on-Chip, an external hybrid integrated device (Chandrasekaran et al. 2007) was proposed initially for the biodetection, wherein, the optical assembly, i.e., the excitation fiber from the laser and the collector fiber to the Spectrometer was hybrid integrated outside the microfluidic domain and the device was used to detect sheep antigen with antisheep antibody tagged with Alexafluor 647. However, the major drawbacks of the externally hybrid integrated device were the optical losses and fiber misalignments, thereby leading to reduced efficiency of fluorescence detection for lower concentrations of the biomolecules.

Even though monolithic fabrication of the waveguides with the microfluidic channels is feasible (Lien et al. 2003; Cohen et al. 2004; Friis et al. 2001; Leeds et al. 2004), optical losses (Splawn and Lytle 2002) incurred in the systems due to scattering, insertion and surface roughness would be detrimental for the detection of low concentration of biomolecules. Therefore, for the present application, the fibers were directly integrated with the microfluidic chip in order to improve the performance of the hybrid integrated system. The proposed opto-microfluidic chip would enable improving the optical coupling efficiency, Q-factor of the fluorescence emission and also minimising the optical losses, such as material absorption loss, scattering loss, etc., thereby creating a robust biophotonic system.

The following sections of the paper give a detailed description of the design and synthesis of the biophotonic chip along with the results of the fluorescence detection experiments.

2 Modeling and design

The schematic illustration of the proposed Lab-on-a-chip system is as shown in Fig. 1. The opto-microfluidic chip basically consists of independent optical and microfluidic channels. The microfluidic setup comprises of inlet/outlet ports and fluidic channels with a detection chamber. In the optical channel, the input fiber from the laser terminates at the detection chamber of the microfluidic channel, to illuminate the fluorescent biomolecules. A collector fiber, which is coupled with the input channel to the Spectrometer-on-Chip, is integrated with the channel at a coupling distance D from the input fiber. It can also be noted that there is a definite offset distance (δ) between the microfluidic channel surface and the core of the optical fibers. Therefore, for a pressure driven flow, when the pressure difference is low between the inlet and the outlet of the channels, flow velocities would be reduced thereby increasing the possibilities of passive immobilization of the biomolecules onto the microfluidic channel surface. It is important to avoid this behaviour as it would hinder biodetection because of the difficulties in the excitation and the emission of fluorescence. Hence, it is very essential that the present biophotonic chip setup has no stagnation flow of biomolecules through suitable microfluidic chamber design.

The Spectrometer-on-Chip, with its size being less than 4 cm^2, is very suitable for integration with the microfluidic device for biophotonic detections. The Spectrometer-on-Chip was designed based on Echelle grating fabricated with Silica-on-Silicon platform (Janz et al. 2004). Herein, the set of input channels, specifically designed for a particular wavelength, terminate at the boundary of slab waveguide region where the light diverges in the waveguide plane and illuminates the grating. Light is diffracted back from the concave grating and is focused onto the output waveguides, which are arrayed along the Rowland circle with a spacing chosen to give the desired channel separation.

One of the novelties of the present work is the wavelength specific configuration of the Spectrometer-on-Chip (Packirisamy et al. 2008) as against the arrangement of a standard spectrometer. Herein, each output channel is designed for specific wavelength of tunable bandwidth targeting fluorescence of a particular band. As there are many output channels available, multiple wavelengths can be detected simultaneously thereby enabling multi-analyte detection. A typical spectral response of a Silica-on-Silicon Spectrometer-on-Chip is given in Fig. 2, in which simultaneous fluorescence at five different wavelengths is detected with as many output channels. In general, the Spectrometer-on-Chip could be designed for many combinations of wavelengths and bandwidths depending upon the application. Hence, the advantage of the Spectrometer-on-Chip is that simultaneous detection of different fluorescent emissions is possible through the different output channels of the chip.

Using similar principle, a 16-channel Spectrometer-on-Chip was designed targeting the fluorescence outputs at specific wavelengths listed in Table 1. The design was

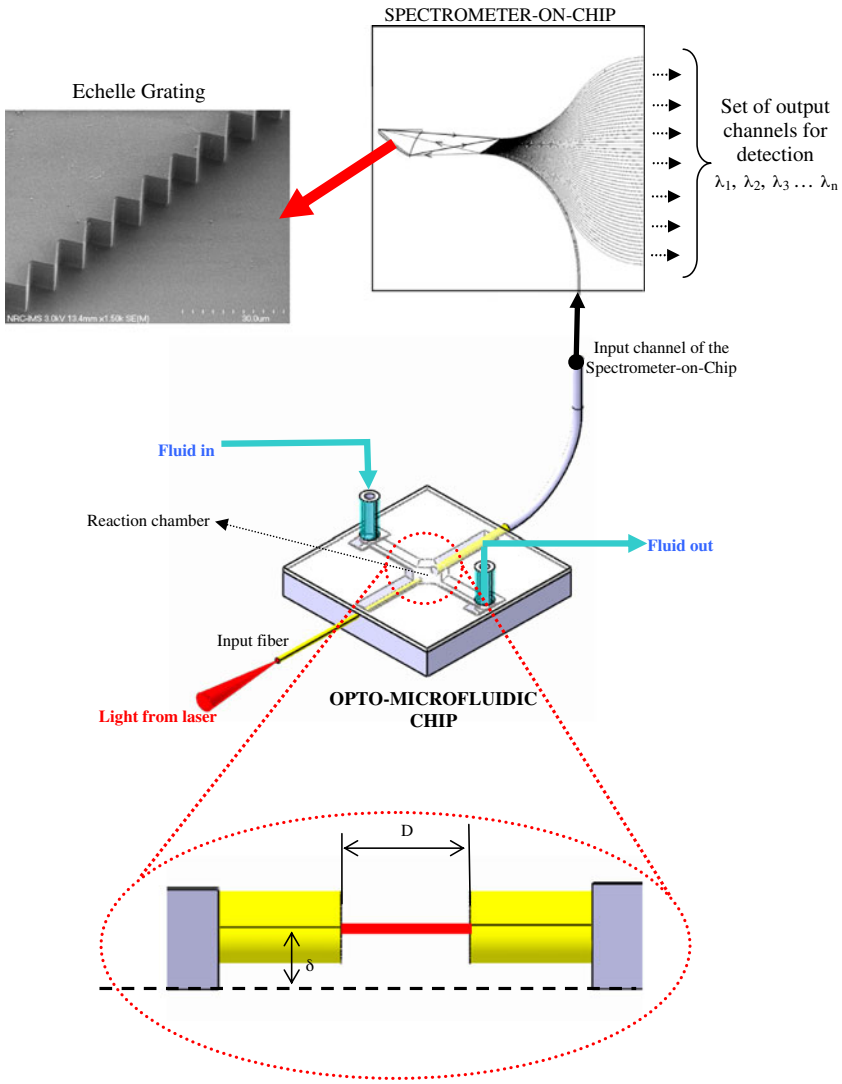

Fig. 1 Schematic illustration of the opto-microfluidic chip integrated with the Spectrometer-on-chip

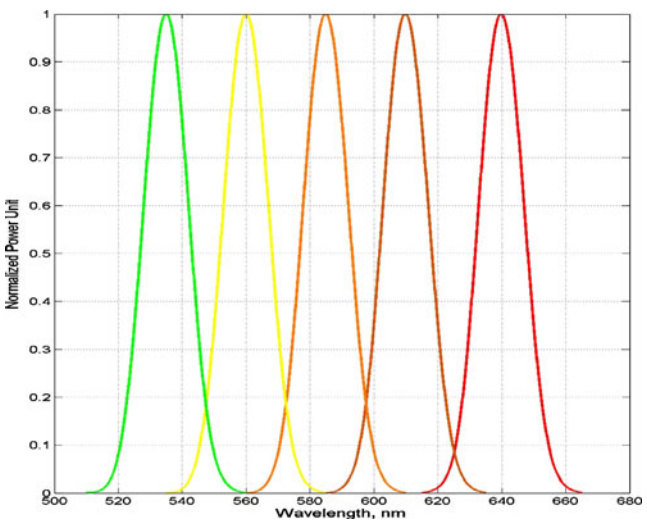

Fig. 2 Typical response (Packirisamy et al. 2008) from the different output channels of the Spectrometer-on-Chip

carried out with a bandwidth of 5–10 nm depending upon the wavelength. For reference, the different channels of the Spectrometer-on-Chip are as listed below, in Table 1.

For the design of the opto-microfluidic chip, several microfluidic channel configurations were considered and

Table 1 Different channels of the Spectrometer-on-Chip and their functions

Channel label	Purpose
Channel 4	Input
Channel 5	Emission at 570 nm(Cy3)
Channel 8	Emission at 550 nm
Channel 9	Emission at 532 nm
Channel 11	Emission at 670 nm (Cy5)
Channel 13	Emission at 650 nm
Channel 14	Emission at 640 nm
Channel 15	Emission at 633 nm

Finite Element Analysis (FEA) was carried out for flow behaviour within the microfluidic chambers. Different geometries of microfluidic channels and detection chambers were modeled using commercial software COMSOL (COMSOL v3.4, http://www.comsol.com) for the Finite Element Analysis by solving the Navier-Stokes equation. Effectively, the modeling and design of the chambers were based on the following criteria:

1. Non-stagnant flow and ease of rinsing
2. Ease of mask preparation for lithography and chip fabrication
3. Relative simplicity of the geometry
4. Ease of integration of optical channels with the microfluidic chip.

Finite Element Modeling of the flow behaviour was carried out for different microfluidic chamber configurations and the results of the analyses showed recirculation of fluid around sharp corners of the chamber under high pressure difference. Hence, optical channels were designed to be away from the fluidic channels with obtuse-angled boundaries. Both these design criteria were satisfied with the selected rhombus geometry of the microchamber.

In the present work, anisotropic etching technique using Tetra Methyl Ammonium Hydroxide (TMAH) was proposed for the fabrication of the opto-microfluidic chip for the following reasons: (a) Ease of fabrication to obtain the desired microchamber geometry, (b) Feasibility of the formation of V-channels for the robust alignment and integration of the optical fibers and (c) Reduced surface roughness. However, this method of fabrication would render an anisotropic chamber geometry due to development of fast etch corners. Therefore, the design of the microchannels and the chambers was carried out in such a way that the micromachined geometry of the chamber is close to the desired shape of the microchamber.

FEA of the flow behaviour within the rhombus chamber were compared with the anisotropic chamber of geometry expected to be obtained using TMAH silicon etching. The results are shown in Fig. 3. It can be seen that the streamlines of flow in both the chambers are very similar.

The flow velocity at the detection zone along the mid streamline, V_{min}, within the microchamber was calculated and results were compared for the anisotropic chamber and the rhombus chamber, assuming a pressure driven flow across the channels. From the graph shown in Fig. 4, it can be seen that there is a very negligible difference between the flow velocities in the stagnant flow zones of rhombus and anisotropic chambers. Thus, through careful design of the chamber, the advantages of the anisotropic etching are utilized without compromising on the flow behaviour.

3 Opto-Microfluidic chip synthesis

Different steps involved in the synthesis of the opto-microfluidic chip include fabrication of the microfluidic chamber, integration of the optical units with the channel, and packaging of optical and microfluidic systems, so as to enable perform integrated microfluidic-bio-photonic detections. In this work, a novel Silicon-Polymer (Polydimethylsiloxane or PDMS) hybrid platform has been developed for the integration of photonic and microfluidic units.

3.1 Fabrication

The feasibilities and advantages of TMAH anisotropic microfabrication for the present work have been outlined in the previous section. In line with those discussions, the following design parameters have been considered for the opto-microfluidic chip:

Width of the optical channel, W_o=250 μm
Width of the microfluidic channel, W_m=150 μm

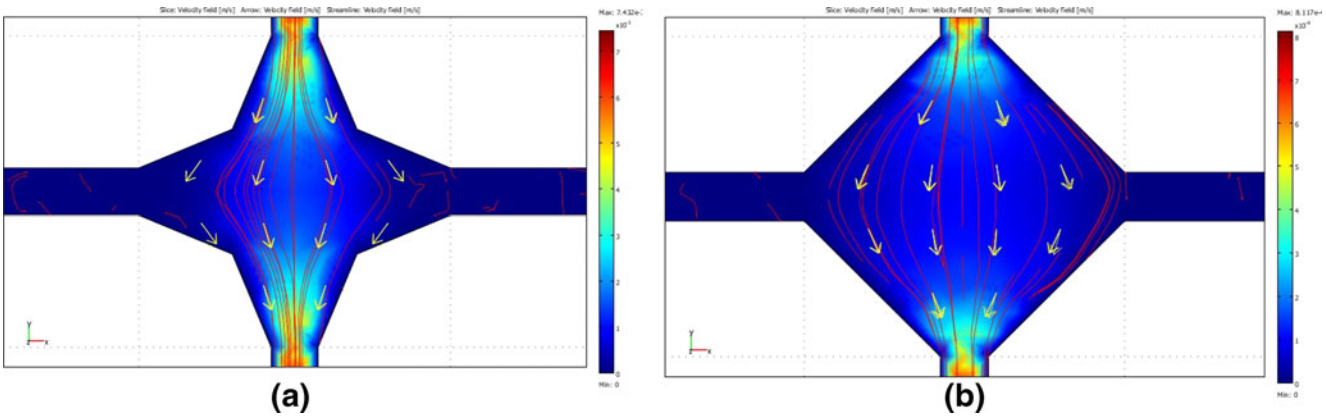

Fig. 3 Results of the finite element analysis of the flow behavior within (**a**) anisotropically etched chamber and (**b**) rhombus chamber

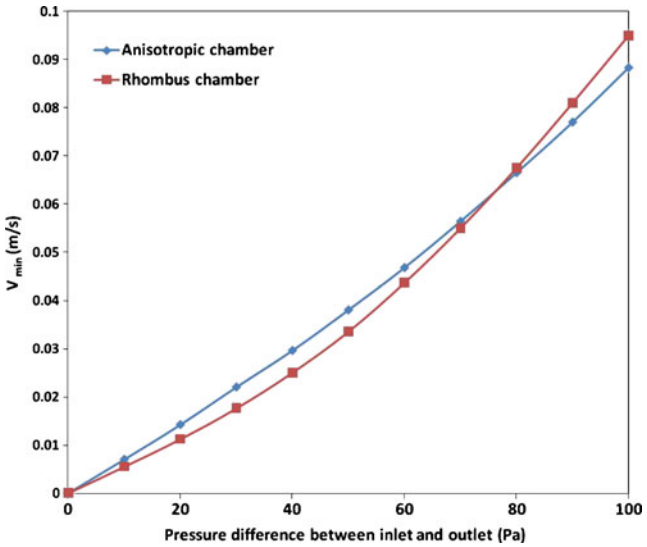

Fig. 4 Comparison of V_{min} in the detection zone of anisotropically etched chamber with rhombus chamber

Width of the Opto-microfluidic chip=25 mm
Wafer thickness=500 μm
Etch time, t: 6 h
Etch rate of 25% TMAH at 80°C along {100}, ER=25 μm/hr
Angle made by the fast etch planes with {100} plane, θ=22.5°
Under Etch Rate (UER) at θ, UER_{max}=58 μm/hr (Landsberger et al. 1996)

The mask design for the microfluidic chamber and the evolution of the chamber geometry during the etching process is as shown in Fig. 5. O is the convex corner in the mask design and O' is the etched corner during etching.

From the design, it can be calculated that under etch rate along OO' is given by

$$UER_{oo'} = \{UER_{max}/\mathrm{Cos}\,\theta\} \quad (1)$$

$$OO'_t = t \times UER_{oo'} \quad (2)$$

Thus, during the etching process the guide length, L, developed for the specified etch time, t is given by

$$L = UER_{max} \times t/\sin\theta \quad (3)$$

For fabicating the chip, 500 μm thick Silicon (100) wafer with an oxide layer thickness of ~500 nm was initially cleaned with Piranha solution made of a 3:1 conc. sulfuric acid (H_2SO_4) with hydrogen peroxide (H_2O_2) for 5 min. Positive photoresist S1813 was spun coated and patterned with a photomask. After developing and post-baking the photoresist, oxide layer was developed with Buffered Oxide Etchant (BOE, 1:6 of 49% HF and 40% NH_4F by volume).

The wafer was then etched in 25% TMAH at 80°C and an etch stop was used for the prevention of back-side etching. The etch rate of <100> silicon obtained under these conditions was 25 μm/hr. The wafer was etched for 6 h and thereafter, rinsed thoroughly with DI water. Oxide layer was subsequently removed. The SEM of the fabricated chamber geometry is as shown in Fig. 6(a). After the fabrication of the chip, the edges were diced as shown in Fig. 6(b) in order to facilitate the integration of fibers with the optical channels.

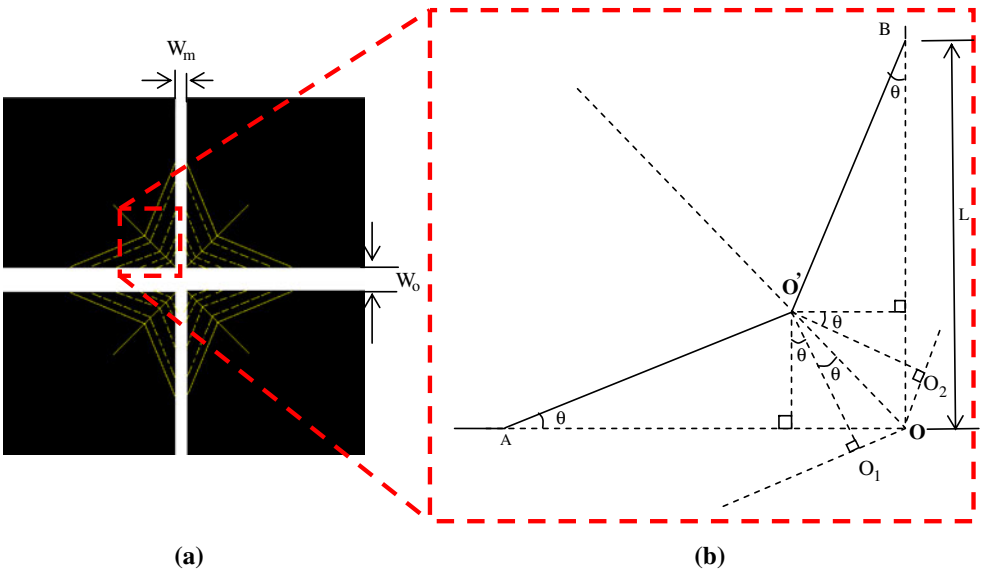

Fig. 5 Schematic diagram showing the etch progress of microchamber. (**a**) Eth mask indicating the etch fronts at four convex corners (**b**) Detailed view of propagation of etch front at a convex corner: O is the convex corner and AO' and BO' are the etch fronts

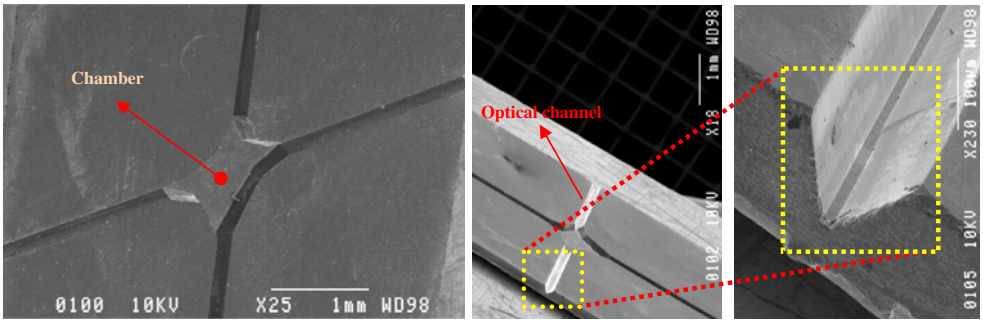

Fig. 6 SEM images of (**a**) fabricated microfluidic chip (**b**) V-slots for fiber integration

3.2 Integration and packaging

FC connectorized tapered lens ended fiber (OZ Optics, ON) connected to a laser was used as the input excitation fiber. Fiber strippers and precision cleavers (Newport, USA) were used to remove buffer layer and cladding around the fiber. The input excitation fiber from the laser source and the output collector fiber coupled to the input channel 4 of the Spectrometer-on-Chip were positioned on the optical channels and supported well so as to isolate them from buckling or bending stresses. In order to determine the coupling distance between the fibers, fiber positioning was carried out under a microscope. The position of the output collector fiber was finely adjusted using a micropositioner for acquiring the maximum optical signal. The fibers were integrated within the optical channel slots using index matching gels and PDMS as shown in Fig. 7, which not only bind the fiber with silicon, but minimize optical losses and also block the channel, thereby preventing leakage of bio-fluid through the optical channels. After the fibers were positioned, UV curable index matching gel (Norland Optical Adhesive 63) was injected into the optical channels and the setup was then cured with UV for 45 s. To complete the sealing, PDMS gel was then coated on top, to enable the bonding of top PDMS cover with the opto-microfluidic chip.

PDMS was chosen as the top cover for the microfluidic channels due to the ease of bulk fabrication, cost-effectiveness and hydrophobicity, which is advantageous for microfluidic lid in order to repel the bio-fluid from adhering onto the surface (Chang et al. 2003). Herein, PDMS was prepared to the required geometry of microfluidic chip by standard soft-lithography process (Xia and Whitesides 1998; Brehmer et al. 2003; McDonald and Whitesides 2002; Rogers and Nuzzo 2005). It was then cleaned in HCl: H_2O solution in the volumetric ratio of 1:5 for 5 min. Two ports (2 mm diameter) were created on the PDMS to form the inlet and outlet of the microfluidic channel. Microfluidic tubes (250 μm inner diameter) were then fitted on the PDMS ports and the setup was again cured at 60°C for 2 h. A thin epoxy layer was coated on the PDMS; it was then aligned with the microfluidic channel and reversibly bonded with the silicon. Another layer of epoxy was then coated around the PDMS silicon interface so that the bonding is leak proof. Figure 8 shows the fully packaged microfluidic chip with integrated input/output waveguides.

4 Spectrometer-on-Chip testing

In order to obtain confidence in the packaging of the Spectrometer-on-Chip with the opto-microfluidic chip, to measure the losses incurred in the system, and to prove the feasibility of using the Spectrometer-on-Chip with the present setup for biological and multi-fluorescence detection applications, the device was tested for the detection of fluorescence from Cy5 dye having an emission peak similar

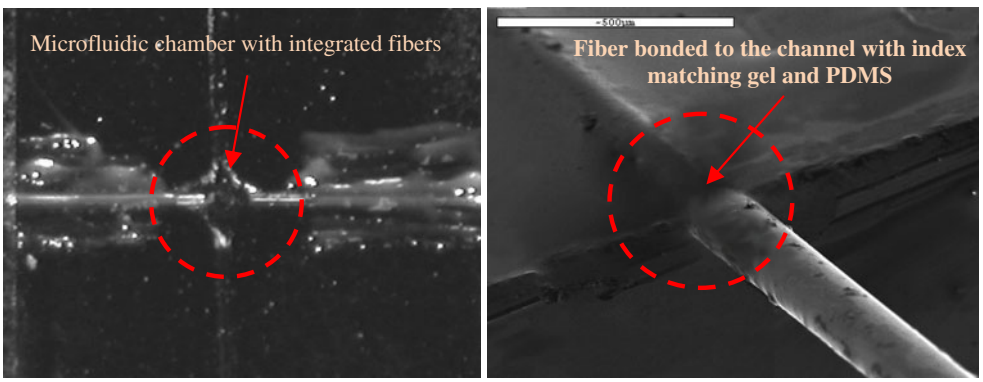

Fig. 7 Integration of fibers with the microfluidic channels

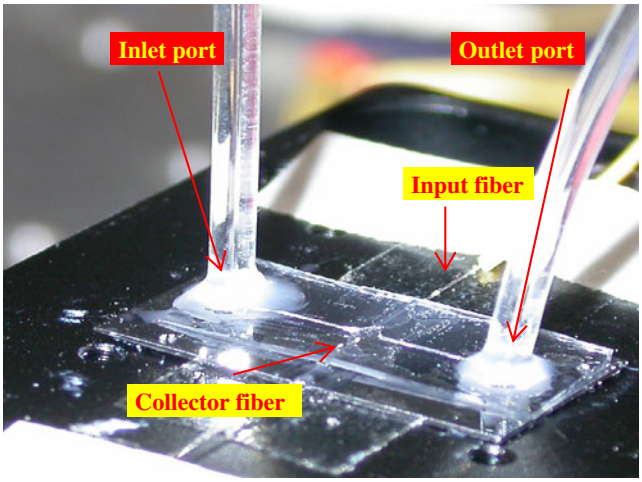

Fig. 8 Fully packaged hybrid biophotonic chip

to Alexafluor 647, at 670 nm. This experiment was carried out under static no-flow conditions of the fluorophore.

Cy5 particles were excited using a laser source at 633 nm, having an optical spectrum as shown in Fig. 9(a). The passband of the grating for Cy5 emission was designed to pick out only the Cy5 emission at 670 nm in channel 11 of the Spectrometer-on-Chip, while filtering out wavelengths outside of the passband, including the excitation wavelength. The device response to the fluorescence excitation at 670 nm from channel 11 is as shown in Fig. 9(b). The measured signal-to-noise ratio is 18.65 dB. From Table 1, it can be seen that channel 15 of the Spectrometer-on-Chip was designed for 633 nm, which is a control channel to confirm the excitation wavelength. Hence, the excitation wavelength at 633 nm was measured from the output channel 15, as shown in Fig. 9(c). Similarly, any number of wavelengths could be detected by proper design of output channels of the Spectrometer-on-Chip as required in the case of multi-analyte detection. Thus, the device was tested for the simultaneous detection of multiple wavelengths. For multi-analyte detection at other wavelengths, the fluorescence emissions can be measured through the optical channels of respective wavelengths, as listed in Table 1. This experiment also provides confidence in employing the Spectrometer-on-Chip with the hybrid integrated setup for measurements under continuous flow conditions.

5 Biophotonic testing

The main objectives of carrying out biophotonic experiments using the opto-microfluidic system were as follows:

(a) To demonstrate the feasibility of real-time biodetection using the integrated microfluidic biophotonic chip
(b) To demonstrate the non-stagnant flow through the microfluidic system
(c) To examine the accuracy of the optical alignment of the system for maximum collection efficiency

Herein, the fluorescence based bio-detection has been demonstrated using Alexafluor 647 tagged anti-sheep antibody as the fluorophore. Five percent antibody (Alexafluor-647, 2 mg/ml, pH7.5 in 0.1 M NaP and 0.1 M NaCl, with 5 mM azide) was prepared by diluting with Phosphate Buffer Solution (PBS). Isopropyl Alcohol (IPA) was used to rinse the microfluidic channel after biodetection.

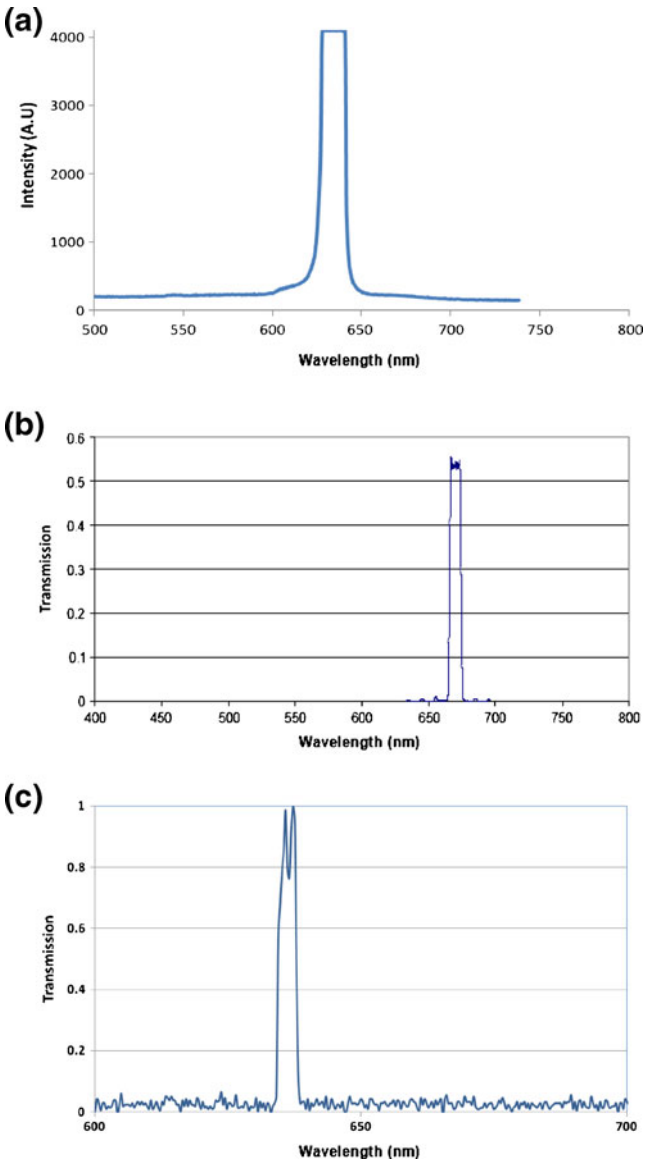

Fig. 9 (**a**) Excitation spectrum from laser source at the input fiber of the microfluidic channel (**b**) Response of the Spectrometer-on-Chip at 670 nm from channel 11 (**c**) Response of the Spectrometer-on-Chip at 635 nm from channel 15

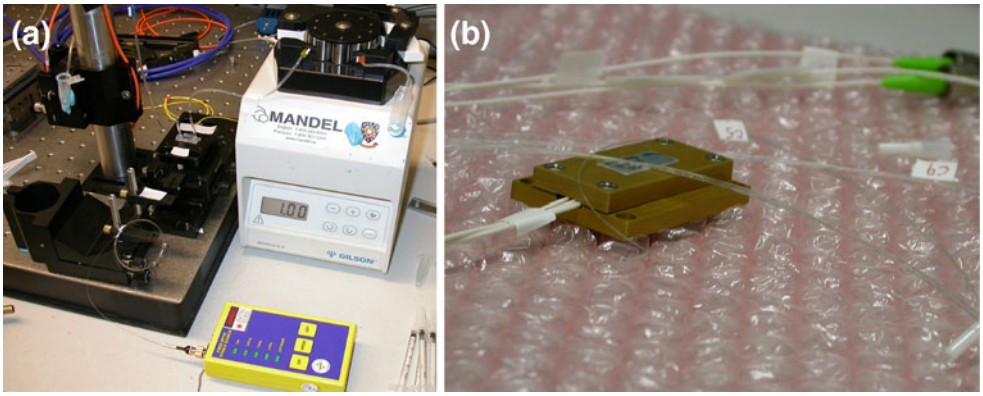

Fig. 10 (**a**) Biodetection testing setup using the integrated device (**b**) Spectrometer-on-Chip

A peristaltic pump (Gilson Minipuls3) was used for fluid injection into the micro-channels. The experimental setup is as shown in Fig. 10. The laser source (OZ Optics) was coupled with the input fiber and the collector fiber was coupled with the Spectrometer-on-Chip. AF647 tagged antibody was pumped into the channel with a peristaltic pump.

The biophotonic testing was carried out in three stages. In the first experiment, the feasibility of biodetection using the integrated system was examined by direct excitation of the fluorophores. Fluorescent signal similar to the signal observed from the Spectrometer-on-Chip for Cy5 was observed, thereby proving that the Spectrometer-on-Chip works well with the integrated opto-microfluidic system. To improve the sensitivity of detection, a multimodal input Spectrometer-on-Chip was used.

The second phase of the biophotonic tests comprised of dynamic microfluidic experiments. These tests were performed in order to demonstrate the feasibility of biophotonic detection using the Spectrometer-on-Chip under continuous flow conditions. In these experiments, a pulsed flow technique was observed wherein, fluorophore tagged antibody molecules were passed into the microfluidic channels for a short duration of 15 s and was rinsed off the channel. The results of the dynamic pulsed flow experiments are presented in Fig. 11. For a Reynolds' number of 1, the residence time, i.e. the time taken by the fluorescent particles to reach the detection zone was ~150 s. The spike in fluorescence is observed at 150 s after the fluorophore tagged antibody molecules enter the detection zone. The experiment was repeated for a pulsed flow for 30 s and the results are shown in Fig. 11(b). The sequence in which the experiment was carried out is given in Table 2, with respect to the experimental results presented in Fig. 11.

From the dynamic experiments, one can observe that there is an immediate increase in the fluorescence signal as soon as the fluorophore enters the reaction chamber at #3 (Fig. 11). Also, the decrease in fluorescence due to the rinsing of the channels beginning at #4 (Fig. 11) is immediate, which shows that the flow in the microfluidic channel is continuous. Therefore, the experimental results prove that the present design of the opto-microfluidic chip is appropriate for non-stagnant flow.

The results of the above experiments were verified for increased concentration of the antibody molecules. Ten

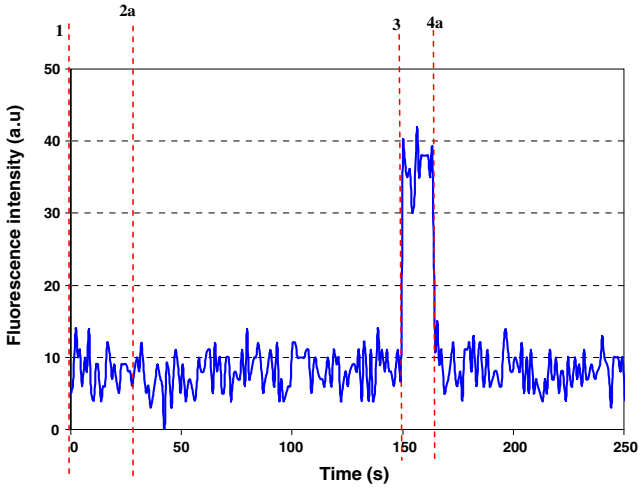

(a) 15s pulsed flow

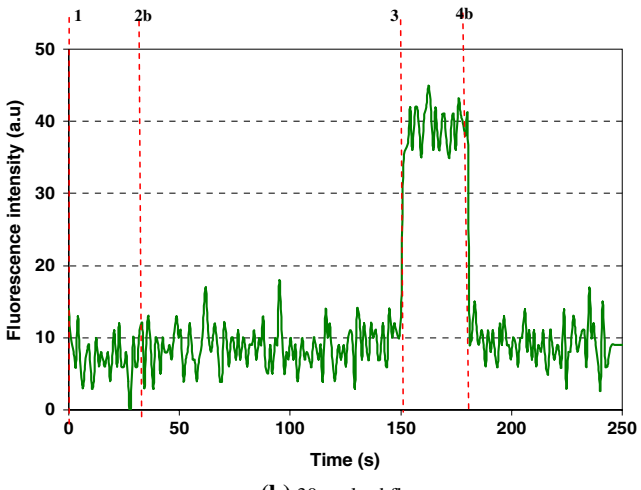

(b) 30s pulsed flow

Fig. 11 Results of dynamic tests with Alexafluor 647 tagged antisheep antibody

Table 2 Sequential procedure for pulsed flow dynamic fluorescence measurement experiments with respect to the results presented in Fig. 11

Step #	Procedure
1	Pass Alexafluor 647 tagged antibody
2	Discontinue the flow of AF647 tagged antibody; pass H2O
3	Fluorophores enter the reaction/detection chamber
4	Fluorophores exit the reaction chamber/rinsing by water begins

* a and b in Fig. 11 indicate the experiments carried out for 15 s and 30 s pulses respectively

percent of 2 mg/ml AF647 tagged antibody was passed continuously through the microfluidic channels using the pulsed flow technique for 15 s and 30 s respectively, and the fluorescence response was verified. The result of the fluorescence detection with higher concentration of AF647 is as shown in Fig. 12. Higher pulse durations were tested for the biodetection feasibilities, however it was observed that for very long pulses, some residual fluorescence was observed.

In order to determine the efficiency of the system for different coupling lengths between the fibers using the same setup, the distance between the input and collector fibers (D) was varied from 250 μm to 2,000 μm. The positioning and the integration of the fibers within the microfluidic chip were carried out under a microscope, and the distance between the fibers was measured under two optical magnifications, based on the field of view. As per the least count of the microscope measurement scale, the positioning precision for the coupling distances of upto 500 μm is ±5 μm and for coupling distances of greater than 500 μm, the positioning precision is ±10 μm.

5% of 2 mg/ml AF647 was passed between the fibers in the microfluidic channel and the fluorescent signals at different coupling distances between the fibers were recorded. The amplitude of the fluorescence signal for each value of D was normalized with respect to the maximum fluorescence observed for L=250 μm. The variation of normalized fluorescence with respect to the coupling distance is shown in Fig. 13.

If τ is the transmission of fluorescent signal into the collector waveguide at any moment, the loss in the system due to the increase in coupling distance is given as

$$\text{Optical loss}, \beta(\text{dB}) = -10\log_{10}\left(\frac{\tau}{\tau_{\max}}\right) \quad (4)$$

Here, τ_{max} is the maximum fluorescent signal at D= 250 μm and τ is the fluorescent signal obtained at any other coupling length. Thus, for the increase in the coupling length from 250 μm to 2,000 μm, the fluorescence loss in the system is 1.1 dB.

The biophotonic experimental results provide confidence in the packaging methods for the synthesis of the integrated device. Through the internal hybrid integration method proposed in this work, low concentration of biomolecules can be detected, which is a major advantage compared with the external hybrid integrated method. The Spectrometer-on-Chip device has enabled in the increase of the quality factor for the fluorescent signals, and the experimental results, shown in Figs. 9, 11 and 12 prove that the device is sensitive for no-flow and continuous flow testing. It is evident that even for an eight fold increase in the coupling distance between the fibers, the relative fluorescent loss is low. This proves that the optical alignment and the optical integration in the system are robust. Thus, the Spectrometer-on-Chip is highly suitable for the integrated microfluidic device for carrying out biophotonic fluorescence detections and can be used in real-time applications for chemical and biological detections.

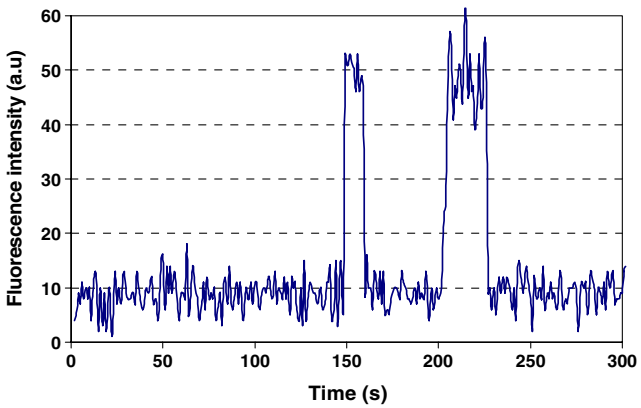

Fig. 12 Results of dynamic tests with 10% of 2 mg/ml AF 647 tagged antisheep antibody

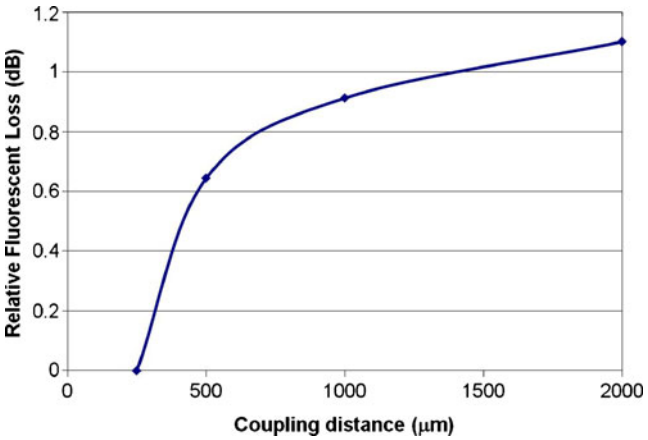

Fig. 13 Variation of the fluorescence loss for different coupling distance between the fibers

6 Conclusion

In this work, an integrated silicon based microfluidic platform was developed for biophotonic detection of fluorescence using a Spectrometer-on-Chip. The feasibility of biodetection has been demonstrated through the successful detection of Alexafluor 647 tagged antibody molecules. The important novelties of the present work are the integration of the Spectrometer-on-Chip with the Opto-microfluidic device, which enables simultaneous detection of multiple fluorescent particles and the hybrid silicon-polymer platform for opto-microfluidic integration. The success of the present work opens up the feasibility of monolithic integration of silicon based microfluidic channel with Silica-on-Silicon based Spectrometer-on-Chip. Other important advantages of the proposed biophotonic system are independence of each module in terms of functionality, multi-analyte detection, rapid, precise and discriminating results with wavelength specific Spectrometer-on-Chip configuration, low background/high signal-to-noise ratio, lack of moving parts, robust, portability, and feasibility of bulk fabrication. Thus, the proposed device is highly suitable for *in-situ* biomedical detections of chemical and biological specimens. Further modifications to the present system would involve monolithic attachment of microfluidic chip and spectrometer to increase the coupling efficiency and study of variation of different microfluidic parameters for improved flow behaviour.

Acknowledgement The authors would like to thank the Canadian Institute for Photonic Innovations (CIPI) and Enablence Inc. for their support in this project. The authors also sincerely thank Mr. Eric Duchesne of Ecole Polytechnique de Montreal for his assistance with the Scanning Electron Microscopy and Mr. Donald Walter Berry of McGill University for his assistance with wafer dicing.

References

P.A. Auroux, D. Iossifidis, D.R. Reyes, A. Manz, Micro total analysis systems. 2. Analytical standard operations and applications. Anal. Chem. **74**, 2637–2652 (2002)

S. Balslev, A.M. Jørgensen, B.B. Olsen, K.B. Mogensen, K.B. Mogensen, D. Snakenborg, O. Geschke, J.P. Kutter, A. Kristensen, Lab-on-a-chip with integrated optical transducers. Lab Chip **6**, 213–217 (2006)

A. Bettiol, E. Teo, C. Udalagama, S.V. Rao, J. van Kan, P. Shao, F. Watt, Integrating photonic and microfluidic structures on a device fabricated using proton beam writing. Proc.of SPIE Vol **6186**, 61860F-1–61860F-8 (2006)

M. Brehmer, L. Conrad, L. Funk, New developments in soft lithography. J. Dispers. Sci. Technol. **24**, 291–304 (2003)

M.A. Burns, B.N. Johnson, S.N. Brahmasandra, K. Handique, J.R. Webster, M. Krishnan, T.S. Sammarco, P.M. Man, D. Jones, D. Heldsinger, An integrated nanoliter DNA analysis device. Science **282**, 484 (1998)

M.L. Chabinyc, D.T. Chiu, J.C. McDonald, A.D. Stroock, J.F. Christian, A.M. Karger, G.M. Whitesides, An integrated fluorescence detection system in poly(dimethylsiloxane) for microfluidic applications. Anal. Chem. **73**, 4491–4498 (2001)

A. Chandrasekaran, A. Acharya, J.L. You, K.Y. Soo, M. Packirisamy, I. Stiharu, A. Darveau, Hybrid integrated silicon microfluidic platform for fluorescence based biodetection. Sensors **7**, 1901–1915 (2007)

W.J. Chang, D. Akin, M. Sedlak, M.R. Ladisch, R. Bashir, Poly (dimethylsiloxane)(PDMS) and silicon hybrid biochip for bacterial culture. Biomed. Microdevices **5**, 281–290 (2003)

D.A. Cohen, J.A. Nolde, C.S. Wang, E.J. Skogen, A. Rivlin, L.A. Coldren, Biophotonic integrated circuits. Proc.SPIE **5594**, 81–93 (2004)

P.S. Dittrich, K. Tachikawa, A. Manz, Micro total analysis systems. Latest advancements and trends. Anal. Chem. **78**, 3887–3908 (2006)

P. Friis, K. Hoppe, O. Leistiko, K.B. Mogensen, J. Hübner, J.P. Kutter, Monolithic integration of microfluidic channels and optical waveguides in silica on silicon. Appl. Opt. **40**, 6246–6251 (2001)

R. Irawan, C.M. Tay, S.C. Tjin, C.Y. Fu, Compact fluorescence detection using in-fiber microchannels-its potential for lab-on-a-chip applications. Lab Chip **6**, 1095–1098 (2006)

S.C. Jakeway, A.J. de Mello, E.L. Russell, Miniaturized total analysis systems for biological analysis. Fresenius J. Anal. Chem. **366**, 525–539 (2000)

S. Janz, A. Balakrishnan, S. Charbonneau, P. Cheben, M. Cloutier, A. Delage, K. Dossou, L. Erickson, M. Gao, P. Krug, Planar waveguide echelle gratings in silica-on-silicon. IEEE Photonics Technol Lett **16**, 503–505 (2004)

L. Jiang, K. P. Gerhardt, B. Myer, Y. Zohar, S. Pau, An SU-8 based fluidic immuno-spectroscopic lab-on-a-chip for rapid quantitative detection of biomolecules. *Micro Electro Mechanical Systems, 2008.MEMS 2008.IEEE 21st International Conference on,* 204–207 (2008)

P. Krulevitch, W. Benett, J. Hamilton, M. Maghribi, K. Rose, Polymer-based packaging platform for hybrid microfluidic systems. Biomed. Microdevices **4**, 301–308 (2002)

L. Landsberger, M. Kharizi, M. Pranjape, On hillocks generated during anisotropic etching of silicon in TMAH. J Microelectromech Syst **5**(2), 106–116 (1996)

A. Leeds, E. Van Keuren, M. Durst, T. Schneider, J. Currie, M. Paranjape, Integration of microfluidic and microoptical elements using a single-mask photolithographic step. Sens Actuators A Phys **115**, 571–580 (2004)

O. Leistiko, P.F. Jensen, Integrated bio/chemical microsystems employing optical detection: the clip-on. J Micromech. Microeng **8**, 148–150 (1998)

V. Lien, Y. Berdichevsky, Y. H. Lo, J. Khandurina, A. Guttman, Monolithic photonics-microfluidics integration for micrototal analysis systems. *Lasers and Electro-Optics, 2003.CLEO'03. Conference on* **4**, (2003)

J.C. McDonald, G.M. Whitesides, Poly (dimethylsiloxane) as a material for fabricating microfluidic devices. Acc. Chem. Res. **35**, 491–499 (2002)

M. Packirisamy, A. Balakrishnan, Planar waveguide based grating device and spectrometer for species-specific wavelength detection. *U.S Patent No. 7324195,* January (2008)

D.R. Reyes, D. Iossifidis, P.A. Auroux, A. Manz, Micro total analysis systems. 1. Introduction, theory, and technology. Anal. Chem. **74**, 2623–2636 (2002)

J.A. Rogers, R.G. Nuzzo, Recent progress in soft lithography. Materials Today **8**, 50–56 (2005)

J.M. Ruano, A. Glidle, A. Cleary, A. Walmsley, J.S. Aitchison, J.M. Cooper, Design and fabrication of a silica on silicon integrated optical biochip as a fluorescence microarray platform. Biosens. Bioelectron. **18**, 175–184 (2003)

B. Samel, V. Nock, A. Russom, P. Griss, G. Stemme, A disposable lab-on-a-chip platform with embedded fluid actuators for active nanoliter liquid handling. Biomed. Microdevices **9**, 61–67 (2007)

J. Seo, L.P. Lee, Disposable integrated microfluidics with self-aligned planar microlenses. Sens Actuators B, Chem **99**, 615–622 (2004)

B.G. Splawn, F.E. Lytle, On-chip absorption measurements using an integrated waveguide. Anal. Bioanal. Chem. **373**, 519–525 (2002)

X.T. Su, K. Singh, C. Capjack, J. Petrcek, C. Backhouse, W. Rozmus, Measurements of light scattering in an integrated microfluidic waveguide cytometer. J. Biomed. Opt. **13**, 024024 (2008)

E. Thrush, O. Levi, W. Ha, K. Wang, S.J. Smith, J.S. Harris, Integrated bio-fluorescence sensor. J. Chromatogr. A **1013**, 103–110 (2003)

T. Vilkner, D. Janasek, A. Manz, Micro total analysis systems. Recent developments. Anal. Chem. **76**, 3373–3385 (2004)

J.R. Webster, M.A. Burns, D.T. Burke, C.H. Mastrangelo, Monolithic capillary electrophoresis device with integrated fluorescence detector. Anal. Chem. **73**, 1622–1626 (2001)

I.M. White, H. Zhu, J. Suter, N.M. Hanumegowda, H. Oveys, M. Zourob, X. Fan, Refractometric sensors for lab-on-a-chip based on optical ring resonators. IEEE Sens. J **7**, 28–35 (2007)

Y. Xia, G.M. Whitesides, Soft lithography. Angew. Chem. Int. Ed. **37**, 550–575 (1998)

S. Yegnanarayanan, W. Roman, M. Soltani, G. Cremona, H. Lu, A. Adibi, On-chip integration of microfluidic channels with ultra-high Q silicon microdisk resonators for lab-on-a-chip sensing applications. in The 20th Annual Meeting of the IEEE Lasers and Electro-Optics Society, 2007, *LEOS*, 50–51 (2007)